Chemosphere 287 (2022) 131977

Contents lists available at ScienceDirect

Chemosphere

journal homepage: www.elsevier.com/locate/chemosphere

Degradation of asbestos – Reinforced water supply cement pipes after a long-term operation

Janez Zavašnik [a,*,1], Andreja Šestan [a,b,1], Srečo Škapin [a]

[a] Jožef Stefan Institute, Jamova Cesta 39, Ljubljana, Slovenia
[b] Jožef Stefan International Postgraduate School, Ljubljana, Slovenia

HIGHLIGHTS

- Deterioration of AC water pipe is seasonal and temperature and pH-dependent.
- Higher water temperature results in calcite scaling, isolating the asbestos from drinking water.
- Lower water temperature cause dissolution of calcite scales and Ca leeching from cement.
- Porous degraded layer is mechanically unstable and results in spallation when subjected to vibrations.
- Cement degradation by calcium leaching is the main reason for asbestos fibres release in drinking water.

ARTICLE INFO

Handling Editor: Junfeng Niu

Keywords:
Asbestos cement
Asbestos fibres
Water pipes
Scaling
Ca leaching
Degradation

ABSTRACT

Potable water supply system in major countries still uses a large proportion of asbestos-cement (AC) pipes for fresh drinking water delivery. Generally, after installation and initial purging, the AC tubes are believed to self-passivate by calcite scale and bio-film, especially when conveying hard water. However, the overall performance of AC tubes after decades of operation is significantly reduced and is still mainly unknown. In the current research, we investigated the AC water supply tube after 56 years of operation with high-hardness conveyed water. Our results show that asbestos fibres are emitted from degraded AC pipes as a result of wall softening due to calcium leaching from hydrated cementitious materials, resulting in the loss of mechanical stability. Although the water pumped into the system is not considered aggressive, the seasonal variations of water temperature and chemistry results in an interplay of calcite scaling and Ca leaching, the latter being the dominating process. By comparing the experimental observations with the long-term chemistry reports of the water supplied through the pipes, a positive relationship was established between the temperature and quality of the conveyed water with the corrosion and the calcite scale formation, which are dictating the emission of the fibres into the drinking water. In addition to the health risks posed by asbestos, these processes have many adverse effects on drinking water supply, such as pipe malfunction and destruction resulting in water loss, reduction of hydraulic capacity, microbial proliferation, and water quality deterioration, a topic of interest for global water industries process.

4. Introduction

Asbestos is a generic commercial designation applied to a group of 6 naturally occurring fibrous silicates: serpentine mineral chrysotile and five amphibole minerals: crocidolite, amosite, anthophyllite, tremolite and actinolite. For much of the 20th-century, asbestos, especially chrysotile (white asbestos) and crocidolite (blue asbestos), was an ingredient in all manner of things, including construction materials (roof shingles, insulation, fireproofing), automotive (brake-pads, gaskets), domestic products, fireproof textiles, etc. (Bartrip, 2004; Dodson and Hammar, 2011). Among others, asbestos-based cement composites (AC), introduced in the late 1920s, were installed worldwide in hundreds of thousands of kilometres of water mains, many still forming a significant component of water distribution networks (Bahadori, 2016; Brandt et al., 2017). AC pipes are made of asbestos fibres, Portland cement and silica, mixed into a slurry and deposited in layers on a

* Corresponding author.
E-mail address: janez.zavasnik@ijs.si (J. Zavašnik).
[1] These authors contributed equally.

https://doi.org/10.1016/j.chemosphere.2021.131977
Received 12 June 2021; Received in revised form 6 August 2021; Accepted 20 August 2021
Available online 24 August 2021

cylindrical mandrel (Ratnayaka et al., 2009). The AC pipes contain varying proportions of asbestos fibres; a typical composition is reported to be about 15–20 wt % asbestos (Benarde, 2018), or about 10–15 vol % (*Cutting, Handling & Disposal of Asbestos Cement (AC) Pipe* Health Canada, 2009; Kelly and Zweben, 2000). For AC mains, only chrysotile and crocidolite were used because of their high strength and chemical inertness to chemical attacks in typical water main applications. The lifespan of AC pipe is estimated at 70 years, but actual service life depends mostly on pipe manufacturing quality and working environments (Punurai and Davis, 2017). Over time, AC pipe undergoes gradual degradation that is influenced by several factors, the most important being the physical characteristic of the AC pipes (age, size, quality of manufacturing), local environment (conveyed water chemistry and aggressiveness of water supply), and operational characteristics (operation, maintenance and repairs) (Hu and Hubble, 2007). Physical and chemical degradation of the AC pipes, especially when conveying aggressive water, detrimentally affect the structural integrity of the AC water mains and can act as a continuous source of asbestos fibres in the drinking water. The ageing of the pipes, leading to pipe softening and increased pipe failures, is also recognised as the important source of asbestos in drinking water (Health Canada, 2009).

The health effects of inhalation of asbestos fibres were identified already in the early 1930s and are nowadays well established (Bartrip, 2004; Boffetta, 1998; Dodson and Hammar, 2011; Doll and Peto, 1985; Lippmann, 2008; McDonald et al., 1971; Murray, 1990). As early as the 1970s, asbestos fibres were also detected in beverages and drinking water (Cunningham and Pontefract, 1971; Murr and Kloska, 1976), but the general opinion on the influence of asbestos fibre ingestion on the digestive tract is still under debate. In the U.S.A., the Environmental Protection Agency under the Safe Drinking Water Act of 1974 has set a maximum asbestos contaminant level of 7 million fibres per litre (U.S. EPA, 2015), while the WHO official guidelines for water safety consider the asbestos ingestion negligible or not to be of prominent concern (Hanley, 2011; World Health Organization, 2011). On the other hand, many studies pointed out the causal effect of ingested asbestos on gastric and colorectal cancer (Bunderson-Schelvan et al., 2011; David Williams, 2013; Di Ciaula and Gennaro, 2016; Varga, 2000), including reports of asbestos in gastrointestinal tissues (Kim et al., 2013), and already abundant medical literature on the topic is rapidly growing. Even though a safe threshold level for asbestos in drinking water is still under discussion in some settings, the veracity of the negative impact of asbestos on public health is well-recognised, and the precautionary principle should impose all possible efforts to revise health policies concerning this topic. In addition, asbestos fibres from drinking water can become airborne via numerous processes such as evaporation during cooking, humidifiers, sprinklers, showering, or from fibres that are trapped on clothing during washing and which are subsequently released into the atmosphere, while in industrial processes these vitalization routes are even more abundant (Webber et al., 1988).

As reported, AC pipes give rise to an increase in the numbers of asbestos fibres in drinking water in some circumstances (Toft et al., 1981; Webber et al., 1989), particularly when first installed or after maintenance (Fawell, 2002); such sporadic release is typically followed by a rapid decrease, suggesting the asbestos presence is independent of the aggressiveness of the water. The suppression of the asbestos release by self-forming inorganic deposits and calciferous scales was observed (Schock and Buelow, 1981), as well as the presence of a biofilm acting as a physical barrier to fibres entering the water ((Istituto Superiore di Sanita) ISS, 1993). Similarly, artificial coating processes serve to bind the asbestos fibres against release but not to seal the cement pipe matrix from dissolution; therefore, indirect observations of increased calcium and pH levels of conveyed water (e.g., carbonate saturation or Langelier Index (Schock, 1984)) do not necessarily indicate fibre release, and AC pipes have to be physically examined (Schock and Buelow, 1981).

Overall, the impact of water on cement and concrete is well documented (Mehta and Monteiro, 2017; Setunge et al., 2009). The asbestos release from AC pipe is possible when one or more of the cement constituents are dissolved and chemically inert asbestos fibres lose their mechanical support. The degree of deterioration of AC pipes depends on the type of cement used and the chemical parameters of the water, such as T and pH, as well as hydrodynamic conditions in water lines (Anderson and Berry, 1981). Furthermore, the addition of disinfectants such as chlorine can cause an increase in pollutants leaching from cement coatings, even in the case of a low disinfectant dose (Młyńska et al., 2019). The asbestos fibres are being released from deteriorated pipes even more abundantly when subjected to vibrations such as road proximity, railroads, construction works, earthquakes, etc. (Ratnayaka et al., 2009).

In light of these risks, an AC pipe condition assessment after a long-term operation is essential to determine their potential for asbestos contamination of drinking water, determine the remaining useful service life, and develop a suitable, proactive replacement plan on time. Thus, in the present study, we investigated the corrosion and scaling process characteristics of AC pipes with conveyed water with high hardness after 56 years of operation. The primary objective of this study was to investigate the dynamics and mechanism of corrosion and the scaling process by material analysis and to establish a possible relationship with water quality parameters and the emission of asbestos fibres from the degraded AC pipe internal surface, which is believed to be absent in hard-water systems. Besides the health risks posed by asbestos, the research is of interest for global water industries due to general adverse effects on drinking water supply such as pipe malfunction and destruction resulting in water loss, reduction of hydraulic capacity, microbial proliferation, and overall water quality deterioration.

5. Material and methods

During the major reconstruction of the drinking water distribution system in the city of Ljubljana, the capital of Slovenia (EU), representative samples of the AC tube mains ($\Phi = 110$ mm), installed in 1963 into the road bedding, were field-collected, rinsed with distilled water, dried at 80 °C in air and preserved in the dust-free container. The samples were collected in the course of several weeks as the reconstruction progressed and were originally part of the same water mains. The reconstruction began due to the ageing of the AC pipes and were replaced by ductile iron pipes (EN 545/ISO 2531).

Scale formation and degradation of the inner surface of the water mains were investigated by scanning electron microscope (SEM, JSM-5800, Jeol) operating at 15 kV. For SEM analysis, sections of the AC tube were cut to 30 × 30 mm samples, mounted onto Al support, and coated with amorphous carbon to increase conductivity. The cross-sections were prepared by dual-beam SEM and focused ion beam microscope (SEM-FIB, Helios NanoLab 650i, FEI), equipped by energy-dispersive X-ray spectrometer (EDS, X'MaX SDD 50 mm^2, Oxford Instruments). To simulate the release of asbestos fibres by mechanical stress and vibrations, parts of degraded AC tube inner surfaces were sonicated in absolute alcohol in an ultrasonic bath (Sonis 4 GT, Iskra PIO), operating at 400 W, 30 kHz, $\lambda = 4023 \times 10^{-2}$ m. All exposed surfaces besides the water-facing side were passivized by thick epoxy-based paint to assure the emission only from the surface in contact with conveyed water. A drop of the solution (70 μl) was pipetted (BRAND®, BRAND GmbH) onto commercially available 200 mesh Ni-supported holey carbon grids (SPI Supplies, Structure Probe Inc.) and investigated in the transmission electron microscope (TEM, JEM-2100, Jeol), operating at 200 kV and equipped with energy-dispersive X-ray spectrometer (EDS, EX-24063JGT, Jeol). The TEM micrographs were recorded by a slow-scan CCD camera (Orius DC1000, Gatan), and a low-background Be double-tilt holder was used for analytics.

Scale formation and corrosion processes are mainly affected by feed water quality such as temperature, pH, hardness, alkalinity, etc.; hence the 10-year data set for the temperature and chemistry of the water was extracted from the public records of the quarterly quality-control tests of

drinking water performed by the National laboratory for health, environment and food. The measured parameters were selected according to the Regulation on drinking water Act (Official Gazette RS, No. 19/04, 35/04, 26/06, 92/06, 25/09, 74/15, 51/17). The results were obtained by the following standards: temperature DIN 38404–4:2000, pH ISO 1052:20,123, electric conductivity EN 27888:1998, sulphate concentration ISO 10304–1:2007, chloride concentration ISO 10304–1:2007, total hardness (°N): ISO 17294–2:2005, Ca ISO 17294–2, Mg ISO 17294–2, Na ISO 17294–2, K ISO 17294–2, Al ISO 17294–2:2003.

6. Results

6.1. Water chemistry

The investigated water distribution system is positioned in the central part of Slovenia and supplies the northern part of the capital city Ljubljana with approx. 36.000 users. The raw water is pumped at water supply station "Šentvid" comprising 3 wells (decimal degrees (DD) coordinates: 46.1013, 14.4808). The water is transported via water mains to reservoir "Pržan", which compensates for daily consumption oscillations (DD: 46.0873, 14.4581). Yearly about 2.5 million m^3 of water is pumped and transported, with an average of 7.000 m^3/day (VO-KA, 2013). The disinfection with chlorine gas is available but has not been used in the past years. In normal operation mode, the water supply system is hydraulically separated and without intermixing with other water sources.

The results of the water quality laboratory tests of the water resource operator (Table 1) are collected in cumulative graphs in Fig. 1 ("Laboratory reports of Central water supply system, 2020"), while the whole dataset can be found in the supplementary file (Table S1). The water temperature in the system varies significantly, from winter 5 °C to summer 20 °C. The pH follows the temperature trend, from about pH = 8 in summer to pH = 7 in winter. From the measured inorganic constituents, $(SO_4)^{2-}$ originates from the geological background. The concentrations follow the seasonal temperature and pH variations and are supposed to be mainly dependent solely on solubility. The sulphate concentrations for neutral or basic (pH > 7.0) soluble sulphates in water that may affect the condition of AC pipe are considered non-aggressive when in the concentration of <150 mg/L; in our analyzed system, the average $(SO_4)^{2-}$ concentration is 12–14 (max. 18) mg/L; hence the possibility of sulphate corrosion attack of AC pipes is negligible and was not considered further. The nitrate (NO_3^-) is related to agricultural influence due to spring fertilization and is legally regulated, although the concentrations remain constant over the years. Similarly, elevated concentrations of chloride (Cl^-) and sodium (Na^+) coincide with the end of the winter and are mainly caused by road salting of the nearby highway network. Due to the low amount of snow in past years, Cl^- and Na^+ concentrations are decreasing and coincide with meteorological data. Potassium appears not to be affected by pH and T variations, and the concentration remains constant over the years. On the other hand, aluminium is rarely found in groundwaters in excess of 10 μg/l, which is in good agreement with the reported values, except for one exceptional reading in the spring of 2016 with a 20 × increase (89 μg/l). Aluminium is to a small amount leached from AC pipes, which reflects in minor seasonal variations; hence such substantial increase is more likely related to the water treatment process, as aluminium compounds are often used as coagulants (Niquette et al., 2004).

Table 1
Analytical results for a water sample, November 7, 2019.

species	Concentration	
	mg/L	mol/L
soluble SiO_2	2.6	0.043272
Ca^{2+}	76.0	1.896302
Mg^{2+}	14.0	0.576013
Na^+	9.0	0.391478
K^+	1.3	0.033249
Cl^-	13.0	0.366683
Al	0.002	0.741×10^{-9}
$(SO_4)^{2-}$	15.0	0.156152
$(NO_3)^-$	16.5	0.266108
$(HCO_3)^-$	295.0	4.834734
conductivity	479 μS/cm	
hardness °N	13.9	
pH	7.4	
T	14.6 °C	

The most critical parameter for assessing the precipitation or degradation of the AC tubes by conveying water is the concentration of Ca^{2+} and Mg^{2+} ions and their ratio; accurate records are available since 2013. The Ca^{2+}/Mg^{2+} ratio is constant over the years (4.5) with three deviations due to exceptionally high Ca^{2+} concentrations and recently due to a significant decrease of Mg^{2+}. As these events are related to unusual behaviour of pH and coincide with the Al-peak artefact, it is safe to assume they result from water treatment procedures.

Based on the water chemistry data we calculated the Langelier Saturation Index (LI), which is used for calculating the ability of a conveyed water to dissolve or deposit calcium carbonate, and is traditionally used to indicate whether conveyed water attacks AC pipe and, if so, its degree of aggressiveness. Langelier index (LI) was calculated as (AWWA Research Foundation, 1996; Langelier, 1936):

$$LI = pH - pH_s \quad [1]$$

where pH is the measured water pH, and pH_s is the pH at saturation in calcite or calcium carbonate. When LI is close to zero, the water is just saturated with calcium carbonate and will neither be strongly corrosive nor scale forming. If the LI value is negative, the water is considered aggressive, and vice-versa, when LI is positive, the water is nonaggressive and scale can form on pipe interior surfaces (Langelier, 1936). For investigated water system, calculated LI is most of the time negative (water is corrosive), but will approach the neutral values during the summer elevated temperatures. Excursions to positive values (scaling will occur) can be observed only when the highest temperatures of conveyed water are achieved, i.e. > 21 °C (Fig. 1 (b)).

6.2. Surface analysis of the water mains

The representative sections of the AC pipe were collected directly from the mains after water switch-off in April 2019. The internal surface of the tube is rough, brownish, and partially porous, homogenous on all sides, and without visible inorganic deposits and traces of the biofilm (Fig. 2, a). Under a stereomicroscope, it is possible to observe the relatively smooth internal surface, with sporadic rougher, grainy patches, while both completely covered by Fe-oxides/hydroxides. The initial secondary electron (SE) SEM observations of the surface revealed exposed inorganic equiaxed particles of about 5 μm or smaller in size (Fig. 2, b), while original intergranular bonding medium appears dissolved, exposing numerous asbestos fibres towards the drinking water side (Fig. 2c and d). The size of the visible fibres is up to several tens of micron, and are consisting of bundles protruding through the surface, with numerous smaller fibres partially embedded.

The inner porous layer, measured from FIB-cut perpendicular into the surface of the tube, extends up to 15 μm in depth (Fig. 3). The surface of the porous layer is covered by a thin layer of Fe-oxides/hydroxides that give the tube a distinctive rusty colour. From the cross-section, we can resolve large, sharp-edged silicate grains about 10 μm in size and smaller rounded grains about 1–1.5 μm in size, apparently not affected by the leaching process and supported by irregular, dendrite-like structures (Fig. 3 b). While the irregularly shaped grains are remains of the original filler, gangue minerals associated with asbestos, and hydrated cementitious matrix (HCM), the grains with rounded cross-section correspond to asbestos fibres bundles which also compose

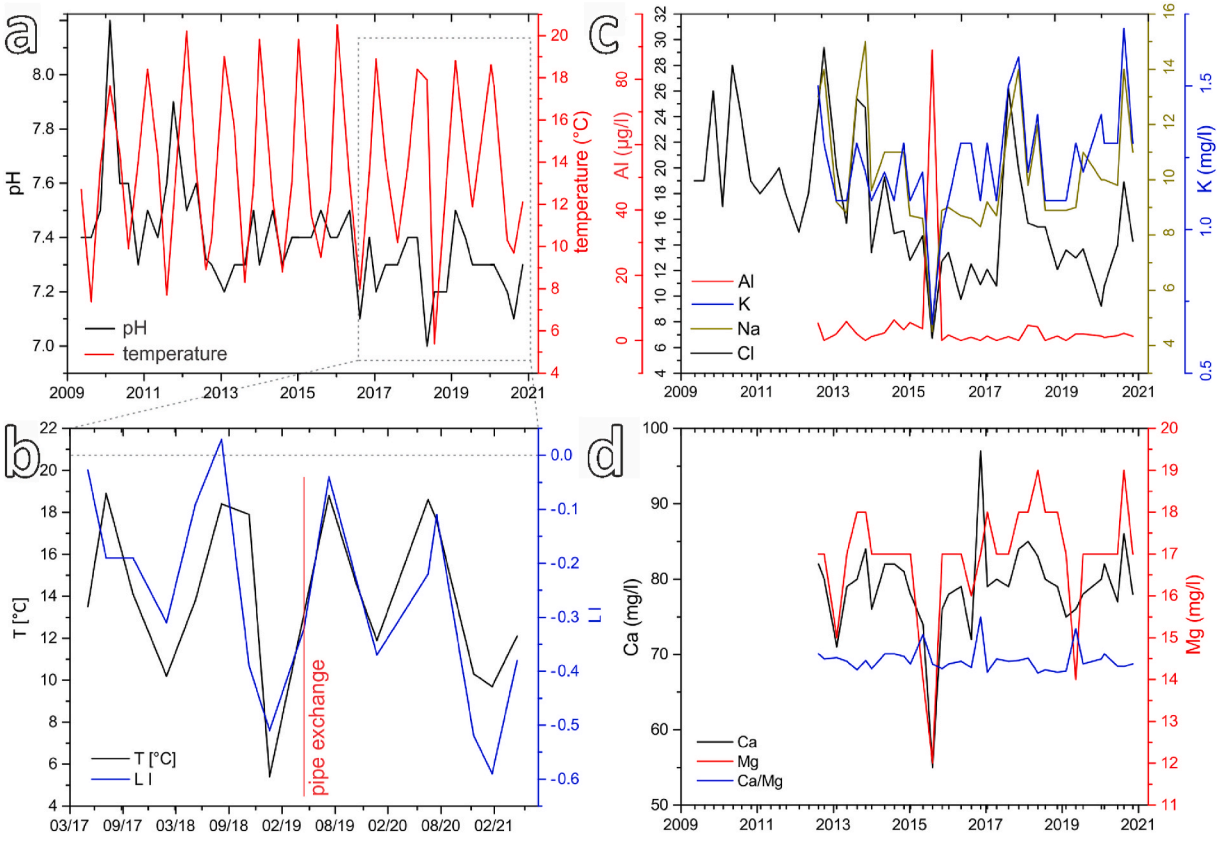

Fig. 1. Cumulative graphs of seasonal variation of (a) temperature and pH, with marked inset of (b) calculated Langelier Saturation Index (LI) and conveyed water temperature (grey horizontal line marks the neutral LI, red vertical line marks the date of pipe exchange, i.e. when samples for surface analysis were taken). Other chemical parameters of the drinking water, where available: (c) Ca^{2+}, Mg^{2+}, and their ratio, and (d) collective graph for Cl, K, Na, and Al seasonal variations. Horizontal base units (x-axis) are date (time-scale) axis, with minor ticks for data points. (For interpretation of the references to colour in this figure legend, the reader is referred to the Web version of this article.)

the majority of the lace-like interconnecting filling between larger cavities. The predominant aggregate in the pipe wall are quartz, dolomite and various alumosilicate mineral grains. Besides Ca dissolution from the binding phase in the tube wall leading to a porous layer in the thickness of about 15 µm, it is expected that other constitutive elements of the binder phase (cement) such as Si and Al will also dissolve.

The most prominent feature is the depletion of calcium throughout the porous section caused by selective leaching. Apparently, calcium is dissolved only from the HCM, while the remaining Ca is chemically bonded to mineral grains that serve as an aggregate, or to asbestos fibres. The Ca-depleted zone ends sharply, but the intergranular clefts and leaching fissures extending to an additional 5 µm in depth (Fig. 3).

To test the mechanical stability and adhesion of the degraded porous layer, the exposed surface of the investigated sample was sonicated for 30 s in pure ethanol in an ultrasonic bath as a proxy variable for years of exposure to vibrations from traffic, construction works or other sources. Afterwards, the surface differs significantly, appears smoother, and the colour changed from light brown to dark grey due to the removal of the superficial Fe-oxides/hydroxides. The sample was dried, embedded in epoxy, ground, and analyzed in SEM in cross-section (Fig. 4). Back-scattered electron (BE) observations and spatial mapping of chemical constituents by EDS shows even distribution without superficial dissolution (Fig. 4, insets). Apparently, the whole 15 µm thick porous layer was removed by sonically-induced vibrations, and only thin about 5 µm thick Ca-depleted zone just beneath the surface can still be detected, similar to in original cross-section just below the porous layer (Fig. 3b). As calcium is leached from cement minerals, the resulting porous structure becomes mechanically unstable and is only poorly attached to the pipe walls.

6.3. Analysis of fibres and particles released from the AC pipe surface

To investigate the possible asbestos release from the degraded inner surface of the AC pipe, a drop of the ethanol solution containing particles released during the sonication of the sample surface was transferred to the TEM support grid. A bright-field transmission electron microscopy (BF-TEM) micrographs revealed numerous fibres up to several microns in length (Fig. 5 a,b). EDS spot analysis (spectra in Fig. 5, e) show typical Mg-rich silicate composition, and the high-resolution (HR) TEM micrographs and associated characteristic selected-area electron diffraction (SAD) ring patterns (Fig. 5, f) correspond to monoclinic clinochrysotile with cell parameter a = 0.53 nm, b = 0.92 nm, c = 1.46 nm, β = 93° (Whittaker, 1956). Most of such nanofibers are terminated by irregular stepped surface induced by crushing or crumbling either during manufacturing, installation, or even during the sample preparation; as asbestos fibrils are hollow and brittle, such nanotubes are easily and frequently broken (Vigliaturo et al., 2019). The analyzed asbestos fibres are all hollow, with about 2:1 wall-to-hole ratio, while the diameter is bimodal with values of 55 ± 2.07 nm and 33 ± 1.13 nm, both having identical chemical composition. Asbestos fibres normally occur in fibril aggregates, but here with a propensity of dispersed single nanotubes due to the ultrasonic dispersion. Besides asbestos, many nano-sized aggregates, either an individual or adjoined with asbestos nanotubes, can be found intermixed (Fig. 5 c, d). By SAD, the aggregates were identified as the Fe-hydroxide – ferrihydrite $(Fe^{3+})_2O_3 \bullet 0.5H_2O$ (Di Giuseppe et al., 2019; Zavašnik et al., 2014).

When looked closely, the fibres are electron-beam sensitive and tend to amorphize in a matter of seconds upon exposure. In our case, the electron dose was restricted by the smallest condenser aperture and

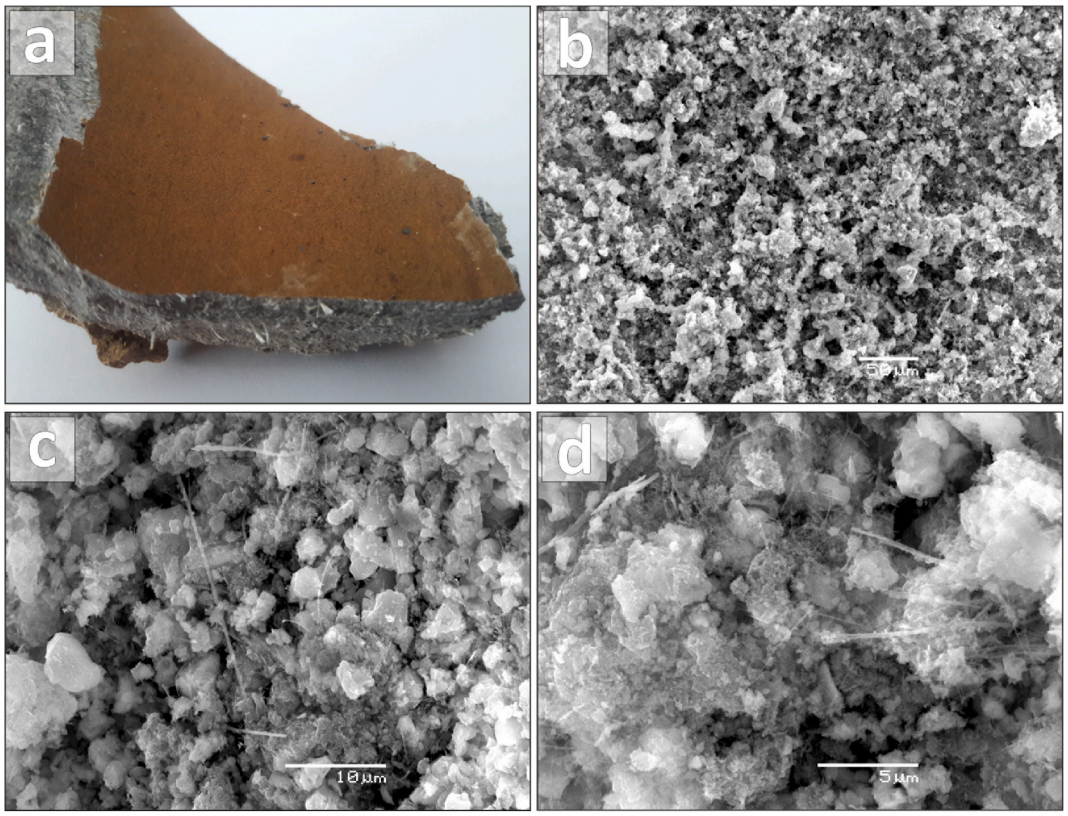

Fig. 2. AC pipe segment with a rough etched surface, covered by Fe-oxides/hydroxides; (a) sections of AC tube collected after reconstruction of the water supply system; (b) SE - SEM micrograph of the inner surface of the AC tube; (c, d) details of the etched pipe surface with loose and partially still embedded asbestos fibres.

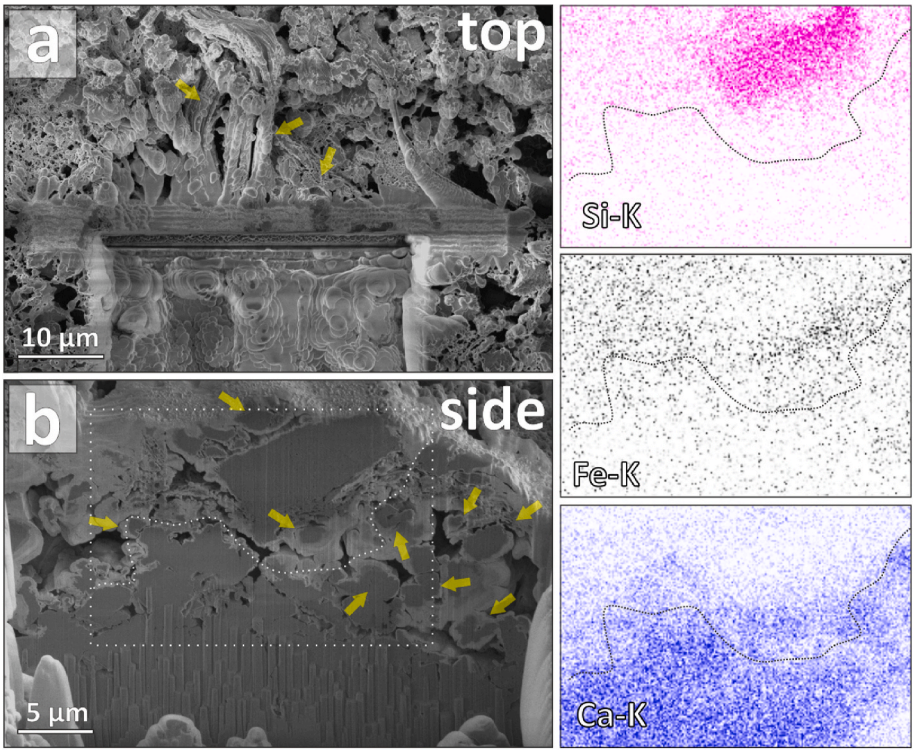

Fig. 3. SE - SEM micrographs of AC pipe surface from (a) top-view of the cross-section, partially altered during protective Pt layer deposition, yellow arrows denote asbestos fibre bundles; (b) side view of the cross-section with corresponding elemental distribution maps for Si, Fe and Ca; the region is marked on (b) with a white dotted square. The auxiliary dotted line in elemental maps is outlining the main transition zone of selective Ca leaching. (For interpretation of the references to colour in this figure legend, the reader is referred to the Web version of this article.)

largest spot size to minimize the irradiation, which resulted in about 180 s of observation time, sufficient for HR-TEM, and subsequent SAD analysis. It is worth mentioning that amorphization will not change the chemical composition significantly; hence EDS analysis was performed last.

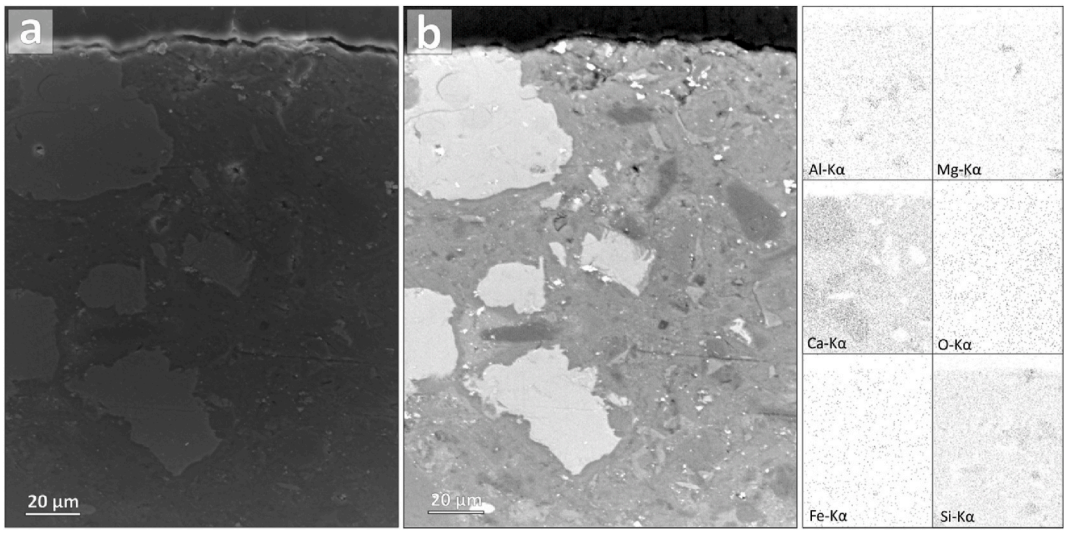

Fig. 4. (a) SE - SEM and (b) BE-SEM micrographs of the sample cross-section after ultrasonic treatment, embedded in epoxy resin (top), followed by AC mixture with several large aggregate grains. Corresponding EDS elemental distribution maps are in the inset, Ca depletion can be observed approx. 5 µm in depth from the top surface.

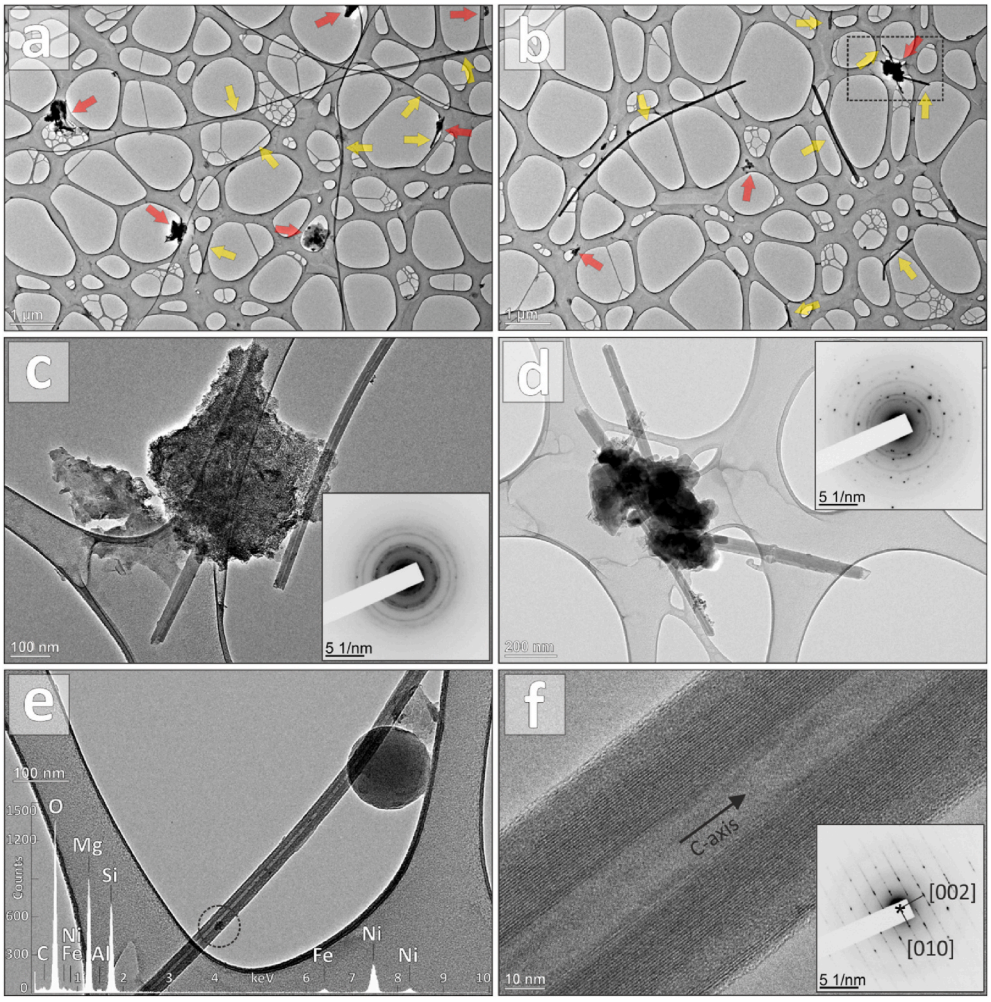

Fig. 5. BF-TEM micrographs of (a, b) multiple asbestos fibres (yellow arrows) and nano-agglomerates (red arrow). (c, d) Fe-hydroxide aggregate embedding asbestos fibres, with corresponding SAD pattern (inset, inverted) characteristic for ferrihydrite. Asbestos fibres are hollow and usually broken. (e) The hollow fibres (tubes) are associated with Fe-hydroxides, and sporadically by nano-plastic spherical particles. Chemical composition corresponds to chrysotile-asbestos (EDS spectra in overprint, the acquisition area is marked with a circle), with additional Ni signal as an artefact from the support grid. (f) HR-TEM micrograph of asbestos nanotube and corresponding SAD pattern (inset, inverted), used for phase identification. (For interpretation of the references to colour in this figure legend, the reader is referred to the Web version of this article.)

6.4. *Residual calcite scale deposition*

While observing the larger sections of the inner surface of the AC pipe, sporadically, several isolated thin islands of inorganic deposit (scale) were observed. Both surfaces, with and without scale, appear the same as are covered by a thin iron oxide layer, and the difference in

morphology can only be observed at high tilt under the stereomicroscope. A section of such scale was cut, and for morphological and chemical characterization, the samples were embedded perpendicularly in epoxy resin, cut, and polished with emery papers until a flat surface was achieved. SEM observations of the cross-section revealed up to 10 μm thick, poorly attached carbonate scale deposited on the etched surface towards the drinking water (Fig. 6a). The top surface of the scale (Fig. 6b) shows cross-section outlines of partially eroded but still recognizable rhombohedral and scalenohedral crystals, a typical morphology for the calcite (Škapin and Sondi, 2010). From the outlines of the scalenohedral cross-sections, we can conclude that the calcite scale is not layered but consist of individual calcite crystals, some of which are intergrown. The layered scaling would imply seasonal deposition, while in our case, observed single-crystals indicate transient deposition. The spallation of the calcite scale due to mechanical stress and drying of the sample can be seen as a sharp, clean crack following the chemical boundary between pure carbonate and partially degraded AC tube. The EDS analysis shows a relative depletion of Al, Mg, and Si in the first 5 μm under the calcite scale (Fig. 6a and b - insets), which is consistent with the surface of the pipe after the sonically-induced vibration treatment (Fig. 4).

7. Discussion

After initial purging, the constant long-term release of asbestos fibres from degrading AC pipes is possible due to selective leaching of the cement binder, especially when the water system is subjected to either constant vibration from traffic or sporadic vibrations during reconstruction, reparation of the water delivery pipes or roadworks when installed into the road bedding (Ratnayaka et al., 2009). The degradation process of the AC is highly complex and is influenced by a large number of factors, including the cement type used in the pipes, the physicochemical quality of the water, and the hydrodynamics of the distribution system. AC pipes were long considered as fairly corrosion-resistant due to natural deposition of protective calcium carbonate scales, especially when conveying hard water, having high mineral content due to percolation through limestone, chalk or gypsum deposits (Anderson and Berry, 1981; Fawell, 2002; Schock, 1984; Schock and Buelow, 1981).

In our investigated system, both scaling and degradation were observed on the surface of AC tubes exposed to the drinking water. The temperature of the transported water is an important parameter affecting the dissolution and precipitation process, and the seasonal fluctuations of up to 15° were measured. As the value for the solubility product varies with temperature and based on analyzed water chemistry, the carbonate scaling was expected, although to a much larger extent. The investigated remains of carbonate scales consist of exclusively calcite ($CaCO_3$) crystals; the most stable form of calcium carbonates and its chemistry and scale formation is well documented and researched (MacAdam and Parsons, 2004). Carbonate in the water system is mainly introduced by the carbonic acid (H_2CO_3) system, which includes the solution of carbon dioxide (CO_2) in water and the formation of carbonic acid, bicarbonate (HCO^-_3) and carbonate (CO^{2-}_3). Unlike most equilibrium systems, the solubility of calcium carbonate increases at lower temperatures; hence the precipitation of calcite is low. The scaling process is mainly dictated by the solubility of CO_2 in the water. As the solubility of CO_2 in the water increases at low temperatures, the concentration of carbonic acid will increase, resulting in a decrease in pH that causes reduced precipitation (Kjellander, 2015). As pH affects the composition of the different carbonates in the carbonic acid system, higher pH also increases carbonate concentration, propagating the precipitation (Frisia, 2006). In the case of the studied system, the pH ranges in a narrow window of pH = 7–8.2, propagating the bicarbonate and, to a lesser extend, carbonic acid. Additionally, just as higher temperature promotes scale formation, higher flow rates further enhance the formation of the scale, which is an important factor in high-throughput systems (Muryanto et al., 2014; Raharjo et al., 2016).

The seasonal variations in water chemistry, temperature, or

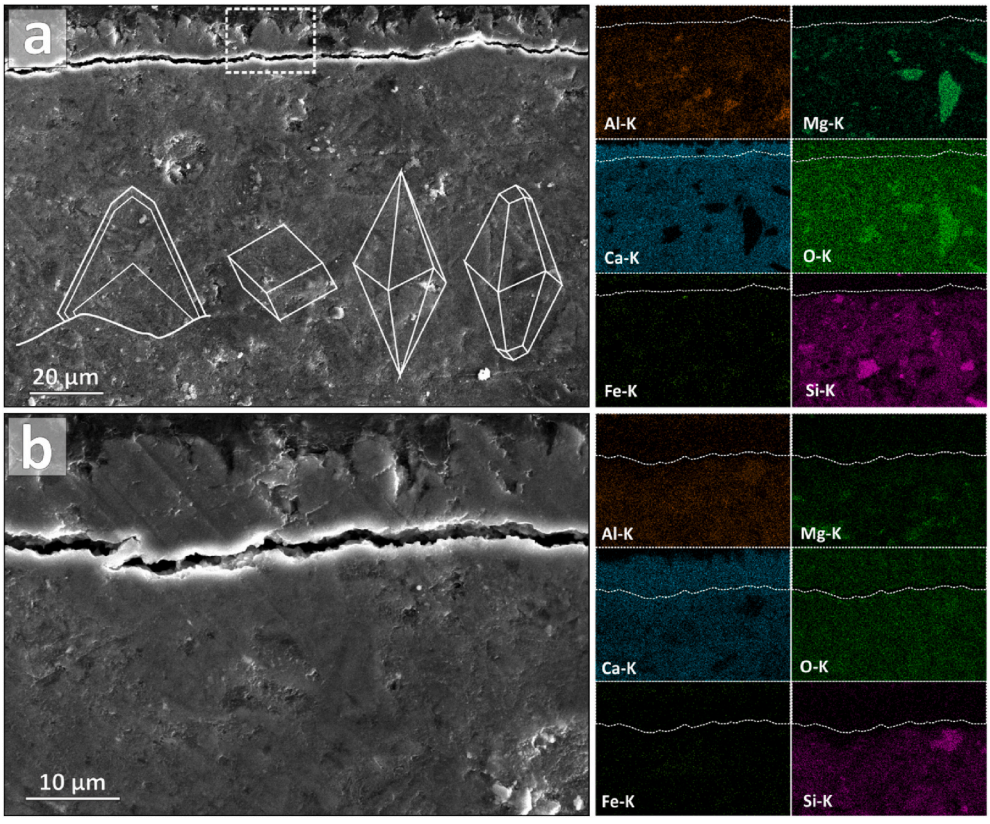

Fig. 6. (a, b) SE - SEM micrographs of the cross-section through the thin calcite scale developed on the surface of AC pipe, with corresponding EDS elemental distribution maps showing depletion of Al, Mg, and Si in the first few μm under the scale. In (a), an outline of a cross-section through typical calcite crystal is overprinted, with a model of calcite rhombohedra, scalenohedra, and combination of both – especially the latter form can be observed on top of the scale. (b) The crack below the calcite layer formed due to poor adhesion during drying of the sample and is superimposed with a white line on the EDS maps.

concentration of contaminants will result in layered scaling depositions (Bum et al., 2015). In our case, the remains of the calcite scale were only a single calcite-crystal-thick, inferring only a limited time of growth. As the investigated pipes were in use for decades, such instant and dramatic changes in water chemistry do not seem plausible. The observation of the degraded sections of the AC tube gives a clue on the possible interplay of the two opposing mechanisms: the scaling deposition of carbonate by precipitation and the opposite mechanism of calcium leaching from the scale dissolution and the AC cement binder. As the inner surface of the AC pipe is mainly deteriorated, and only several isolated calcite islands were found, it is safe to conclude the Ca dissolution is the dominant process.

The AC tubes degradation by the dissolution of solid Ca in cement hydrates when exposed to water is governed by solubility and kinetic properties of the materials involved (Safe Drinking Water Committee; Board on Toxicology and Environmental Health Hazards; Niquette et al., 2004). The cement matrix of the AC pipe is a complex system of more than 100 compounds and phases. The hydrated cementitious matrix (HCM) makes up the backbone of concrete strength and durability, with calcium-silicate-hydrates (C–S–H) as its main constituent. The C–S–H is extremely variable and poorly ordered phase composed of mainly hydrated C_2S and C_3S (Richardson, 2008) with a stable microstructure at a pH range of 9.0–10.0 (Taylor, 1997), while environments with a lower pH have the capacity to break down the C–S–H by calcium ions removal (Bertron et al., 2005). In the studied system, the pH varies between 7 and 8.2, acting corrosively towards the C–S–H. As the Ca leaching from the AC pipe is governed by solubility considerations and the quality of the water in contact with the AC pipe, having a substantial impact on the rate at which the dissolution reaction occurs. Possible dissolution reactions in AC by following reactions increase pH, calcium, and alkalinity of water in contact with the pipe (Schock and Buelow, 1981):

$$Ca(OH)_2(s) \quad => \quad Ca^{2+} + 2OH^- \qquad [2]$$

$$Ca_3SiO_5(s) + 5H_2O \quad => \quad 3Ca^{+2} + H_4SiO_4^0 + 6OH^- \qquad [3]$$

$$Ca_2SiO_4\ (s) + 4H_2O \quad => \quad 2Ca^{+2} + H_4SiO_4^0 + 4OH^- \qquad [4]$$

$$Ca_3Al_2O_6(s) + 6H_2O \quad => \quad 3Ca^{+2} + 2Al^{+3} + 12OH^- \qquad [5]$$

We have to mention that C_3S, C_2S and C_3A are phases before hydratization; in the concrete they are hydrated, e.g. C_3S with water produces $C_3S_2H_3$, which corresponds to $Ca_3Si_2O_7{\cdot}3H_2O$.

Analysis of the results showed that there is no simple model to explain degradation measured by elemental analysis of the AC tubes and initial data on the water chemistry due to several interfering factors. Firstly, the conveyed water is subjected to treatment, which can have a substantial effect even when minor concentrations are used. Additional factors affecting correlation are the place of AC pipes manufacture, the cement type, additional coating delaying the chemical attack, the abrasive properties of the water, and changes in treatment during long-term operation. In most cases, these parameters are not quantifiable and may interfere with other results and statistical analysis. Therefore, estimating the potential rate of asbestos fibres released into the drinking water is extremely difficult and requires physical examination of the pipe samples. Additionally, when large fluctuations of, e.g., temperature are present, the sampling must be performed at different time intervals during the temperature oscillation.

The emission of asbestos fibres into the drinking water as a result of degradation of the AC pipes is therefore related to internal surface area (tube diameter) and proportional to the rate at which the degradation is proceeding, while the removal of fibres is by water flow conditions and is transient in nature. The general trend is that AC pipes are vulnerable to attack where conveyed water alkalinity is below 75 mg/l or the pH below 7.5 (AWWA Research Foundation, 1996). The cement phase of AC pipes is composed of up to 38–65% of calcium oxide, and until calcium equilibrium between cement and the conveyed water is reached, Ca from the cement will be either leached out of or precipitated into the cement pores, depending on the precipitation potential of the water (Taylor, 1997). On the other hand, even when conveying hard water, pipe degradation can be mitigated but still has to be considered in terms of long-term operation.

As the AC pipes indeed present the sporadic source of asbestos fibres when subjected to malfunction and repair and at the same time, calcium leaching is degrading the structural components of the AC tube, releasing the asbestos fibres into the drinking water - the process is even faster when such pipe is subjected to mechanical vibrations due to traffic, construction or other sources.

8. Conclusions

The analysis of the AC tube after decades-long operation revealed surface corrosion as a result of Ca leeching from the pipe wall. The conveyed water is aggressive towards AC pipes during winter period and approaches neutral values during summer, with sporadic scaling formation at the peak water temperatures over 21 °C.

- The presence of asbestos fibres in potable water distribution systems results from degradation of the AC pipe after a long-term operation,
- For investigated water system, conveyed water is most of the time considered corrosive, but will approach the neutral values during the summer elevated temperatures. Carbonate scaling occurs only at the highest conveyed water temperatures >21 °C,
- Asbestos fibres are released from corroded AC pipe at an accelerated rate when subjected to vibrations,
- Rate of corrosive attack is suppressed by seasonal precipitation of calcite scale,
- The thickness of the porous layer resulting from Ca leaching is 20 μm, while maximum internal degradation in a period of 50+ years cannot be established,
- The release of fibres into the water supply may pose a health risk to those who drink and use such water.

Funding

This project has received funding from the European Union's Horizon 2020 research and innovation programme under grant agreement No 823717 –ESTEEM3.

Conflicts of interest/Competing interests

The authors declare that they have no known competing financial interests or personal relationships that could have appeared to influence the work reported in this paper.

Availability of data and material

Electronic Supplementary Information (ESI) is available from a public repository: J. Zavašnik et al. (2020) Water quality dataset - Degradation of asbestos – reinforced water supply cement pipes after a long-term operation, https://doi.org/10.17632/8d9wr6sdtg.1.

Code availability

Not applicable.

Credit author statement

Janez Zavašnik - Conceptualization, Formal analysis, Writing - Original Draft, Andreja Šestan - Conceptualization, Formal analysis, Writing - Original Draft, Srečo Škapin - Methodology, Writing - Review & Editing, Supervision.

Declaration of competing interest

The authors declare that they have no known competing financial interests or personal relationships that could have appeared to influence the work reported in this paper.

Acknowledgements

JZ acknowledges the support from the European Union's Horizon 2020 research and innovation programme under grant agreement No 823717 – ESTEEM3.

Appendix A. Supplementary data

Supplementary data associated with this article can be found, in the online version, at https://doi.org/10.1016/j.chemosphere.2021.131977.

References

Anderson, R., Berry, D., 1981. Regulating corrosive water. Water Resour. Res. 17, 1571–1577. https://doi.org/10.1029/WR017i006p01571.
AWWA Research Foundation, 1996. Internal Corrosion of Water Distribution Systems. American Water Works Association, ISBN 0898677599.
Bahadori, A., 2016. Water supply and distribution systems. Essentials Oil Gas Util 225–328. https://doi.org/10.1016/b978-0-12-803088-2.00008-0.
Bartrip, P.W.J., 2004. History of asbestos related disease. Postgrad. Med. 80, 72–76. https://doi.org/10.1136/pmj.2003.012526.
Benarde, M.A. (Ed.), 2018. Asbestos the Hazardous Fiber. CRC Press, Boca Raton, ISBN 9781315890821.
Bertron, A., Duchesne, J., Escadeillas, G., 2005. Attack of cement pastes exposed to organic acids in manure. Cement Concr. Compos. 27, 898–909. https://doi.org/10.1016/j.cemconcomp.2005.06.003.
Boffetta, P., 1998. Health effects of asbestos exposure in humans: a quantitative assessment. Med. Lav. 89, 471–480.
Brandt, M.J., Johnson, K.M., Elphinston, A.J., Ratnayaka, D.D., 2017. Chemistry, microbiology and biology of water. Twort's Water Supply 235–321. https://doi.org/10.1016/b978-0-08-100025-0.00007-7.
Bum, M., Kim, J., Dockko, S., 2015. LSI characteristics based on seasonal changes at water treatment plant of Korea. Desalin. Water Treat. 55, 272–277. https://doi.org/10.1080/19443994.2014.912963.
Bunderson-Schelvan, M., Pfau, J.C., Crouch, R., Holian, A., 2011. Nonpulmonary outcomes of asbestos exposure. J. Toxicol. Environ. Health B Crit. Rev. 14, 122–152. https://doi.org/10.1080/10937404.2011.556048.
Cunningham, H.M., Pontefract, R., 1971. Asbestos fibres in beverages and drinking water. Nature 232, 332–333. https://doi.org/10.1038/232332a0.
David Williams, S.J.K., 2013. Asbestos-induced gastrointestinal cancer: an update. J. Gastrointest. Dig. Syst. 3 https://doi.org/10.4172/2161-069x.1000135.
Di Ciaula, A., Gennaro, V., 2016. Rischio clinico da ingestione di fibre di amianto in acqua potabile. Epidemiol. Prev. 40, 472–475. https://doi.org/10.19191/EP16.6.P472.129.
Di Giuseppe, D., Zoboli, A., Vigliaturo, R., Gieré, R., Bonasoni, M.P., Sala, O., Gualtieri, A.F., 2019. Mineral fibres and asbestos bodies in human lung tissue: a case study. Minerals 9, 1–21. https://doi.org/10.3390/min9100618.
Dodson, R.F., Hammar, S.P., 2011. Asbestos: Risk Assessment, Epidemiology, and Health Effects. CRC press, ISBN 9781138076709.
Doll, R., Peto, J., 1985. Effects on Health of Exposure to Asbestos. Applied Optics. Health & Safety Commission. https://doi.org/10.1364/AO.40.004376.
Fawell, J.K., 2002. Asbestos Cement Drinking Water Pipes and Possible Health Risks, vol. 44.
Frisia, S., 2006. Calcium carbonate and the carbonic acid system. Geochemistry 51–57. https://doi.org/10.1007/1-4020-4496-8_39.
Hanley, D.G., 2011. Toxicological Profile for Asbestos, Agency for Toxic Substances and Disease Registry. DIANE Publishing. https://doi.org/10.1201/9781420061888_ch34.
Health Canada, 2009. Guidance on controlling corrosion in drinking water distribution systems. Water, Air and Climate Change Bureau, Healthy Environments and Consumer Safety Branch, Health Canada, Ottawa, Ontario, Ottawa.
Hu, Y., Hubble, D.W., 2007. Factors contributing to the failure of asbestos cement water mains. Can. J. Civ. Eng. 34, 608–621. https://doi.org/10.1139/L06-162.
ISS (Istituto Superiore di Sanita), 1993. Research Project, Rome.
Kelly, A., Zweben, C. (Eds.), 2000. Comprehensive Composite Materials. Pergamon, ISBN 9780080429939.
Kim, S.J., Williams, D., Cheresh, P., Kamp, D.W., 2013. Asbestos-induced gastrointestinal cancer: an update. J. Gastrointest. Dig. Syst. 3 https://doi.org/10.4172/2161-069x.1000135.
Kjellander, M., 2015. Formation and Prevention of Calcite Scale at Dåvamyran. Degree Project in Engineering Chemistry. Department of Chemistry, Umeå Universitet, Sweden.
Laboratory Reports of Central Water Supply System [WWW Document], 2020. URL. https://www.vokasnaga.si/pitna-odpadna-voda/kaksno-vodo-pijemo/centralni-vodovodni-sistemi/arhiv/sentvid.
Langelier, W.F., 1936. The analytical control of anti-corrosion water treatment. J. Am. Water Works Assoc. 28, 1500–1521. https://doi.org/10.1002/J.1551-8833.1936.TB13785.X.
Lippmann, M., 2008. Environmental Toxicants: Human Exposures and Their Health Effects, third ed. John Wiley & Sons. https://doi.org/10.1002/9780470442890. Environmental Toxicants: Human Exposures and Their Health Effects: Third Edition.
MacAdam, J., Parsons, S.A., 2004. Calcium carbonate scale formation and control. Rev. Environ. Sci. Biotechnol. 3, 159–169. https://doi.org/10.1007/s11157-004-3849-1.
McDonald, J.C., McDonald, A.D., Gibbs, G.W., Siemiatycki, J., Rossiter, C.E., 1971. Mortality in the chrysotile asbestos mines and mills of quebec. Arch. Environ. Health 22, 677–686. https://doi.org/10.1080/00039896.1971.10665923.
Mehta, P.K., Monteiro, P.J.M., 2017. Concrete Microstructure, Properties and Materials, ISBN 0071797874.
Młyńska, A., Zielina, M., Bielski, A., 2019. Contamination of drinking water soon after cement mortar lining renovation depending on the disinfectant doses. SN Appl. Sci. 1, 1–9. https://doi.org/10.1007/s42452-019-0507-3.
Murr, L.E., Kloska, K., 1976. The detection and analysis of particulates in municipal water supplies by transmission electron microscopy. Water Res. 10, 469–477. https://doi.org/10.1016/0043-1354(76)90066-X.
Murray, R., 1990. Asbestos: a chronology of its origins and health effects. Br. J. Ind. Med. 47, 845.
Muryanto, S., Bayuseno, A.P., Ma'mun, H., Usamah, M., Jotho, 2014. Calcium carbonate scale formation in pipes: effect of flow rates, temperature, and malic acid as additives on the mass and morphology of the scale. Procedia Chem 9, 69–76. https://doi.org/10.1016/j.proche.2014.05.009.
Niquette, P., Monette, F., Azzouz, A., Hausler, R., 2004. Impacts of substituting aluminum-based coagulants in drinking water treatment. Water Qual. Res. J. Can. 39, 303–310. https://doi.org/10.2166/wqrj.2004.041.
Punurai, W., Davis, P., 2017. Prediction of asbestos cement water pipe. Aging and Pipe Prioritization using Monte Carlo Simulation 21, 1–13. https://doi.org/10.4186/ej.2017.21.2.1.
Raharjo, S., Bayuseno, A., Jamari, Muryanto S., 2016. Calcium carbonate scale formation in copper pipes on laminar flow. MATEC Web Conf 58. https://doi.org/10.1051/matecconf/20165801029.
Ratnayaka, D.D., Brandt, M.J., Johnson, K.M., 2009. Pipeline design and construction. Water Supply 561–598. https://doi.org/10.1016/b978-0-7506-6843-9.00023-8.
Richardson, I.G., 2008. The calcium silicate hydrates. Cement Concr. Res. 38, 137–158. https://doi.org/10.1016/j.cemconres.2007.11.005.
Schock, M.R., 1984. Temperature and ionic strength corrections to the langelier index - revisited. J. Am. Water Works Assoc. 76, 72–76. https://doi.org/10.1002/j.1551-8833.1984.tb05391.x.
Schock, M.R., Buelow, R.W., 1981. Behavior of asbestos-cement pipe under various water quality conditions - 2. Theoretical considerations. J. Am. Water Works Assoc. 73, 636–651. https://doi.org/10.1002/j.1551-8833.1981.tb04827.x.
Setunge, S., Nguyen, N., Alexander, B.L., Dutton, L., 2009. Leaching of alkali from concrete in contact with waterways. Water, air, soil pollut. Focus 9, 381. https://doi.org/10.1007/s11267-009-9234-x.
Škapin, S.D., Sondi, I., 2010. Synthesis and characterization of calcite and aragonite in polyol liquids: control over structure and morphology. J. Colloid Interface Sci. 347, 221–226. https://doi.org/10.1016/j.jcis.2010.03.070.
Taylor, H.F.W., 1997. Cement Chemistry, Cement Chemistry. Thomas Telford Publishing. https://doi.org/10.1680/cc.25929.
Toft, P., Wigle, D., Meranger, J.C., Mao, Y., 1981. Asbestos and drinking water in Canada. Stud. Environ. Sci. 12, 77–89. https://doi.org/10.1016/S0166-1116(08)70840-9.
U.S. EPA, 2015. Summary of the safe drinking water act [WWW document], 8.2.21. https://www.epa.gov/laws-regulations/summary-safe-drinking-water-act.
Varga, C., 2000. Asbestos fibres in drinking water: are they carcinogenic or not? Med. Hypotheses 55, 225–226. https://doi.org/10.1054/mehy.2000.1049.
Vigliaturo, R., Pollastri, S., Gieré, R., Gualtieri, A.F., Drazić, G., 2019. Experimental quantification of the Fe-valence state at amosite-asbestos boundaries using acSTEM dual-electron energy-loss spectroscopy. Am. Mineral. 104, 1820–1828. https://doi.org/10.2138/am-2019-7218.
VO-KA, 2013. Program oskrbe s pitno vodo za obdobje 2014 - 2017. Javno podjetje Vodovod - Kanalizacija d.o.o.
Webber, J.S., Covey, J.R., King, M.V., 1989. Asbestos in drinking water supplied through grossly deteriorated A-C pipe. J. Am. Water Works Assoc. 81, 80–85. https://doi.org/10.1002/j.1551-8833.1989.tb03167.x.
Webber, J.S., Syrotynski, S., King, M.V., 1988. Asbestos-contaminated drinking water: its impact on household air. Environ. Res. 46, 153–167. https://doi.org/10.1016/S0013-9351(88)80029-X.
Whittaker, E.J.W., 1956. The structure of chrysotile. II. Clino-chrysotile. Acta Crystallogr. 9, 855–862. https://doi.org/10.1107/s0365110x5600245x.
World Health Organization, 2011. Guidelines for Drinking-Water Quality, fourth ed., vol. 38. WHO chronicle, Geneva, ISBN 978 92 4 1548151.
Zavašnik, J., Stanković, N., Arshad, S.M., Rečnik, A., 2014. Sonochemical synthesis of mackinawite and the role of Cu addition on phase transformations in the Fe-S system. J. Nanoparticle Res. 16 https://doi.org/10.1007/s11051-013-2223-z.